



OPEN

Agreement and precision of wide and cube scan measurements between swept-source and spectral-domain OCT in normal and glaucoma eyes

Huiyuan Hou¹✉, Nevin W. El-Nimri¹, Mary K. Durbin¹, Juan D. Arias¹, Sasan Moghimi² & Robert N. Weinreb²

This study aimed to evaluate agreement of Wide scan measurements from swept-source optical coherence tomography (SS-OCT) Triton and spectral-domain OCT (SD-OCT) Maestro in normal/glaucoma eyes, and to assess the precision of measurements from Wide and Cube scans of both devices. Three Triton and three Maestro operator/device configurations were created by pairing three operators, with study eye and testing order randomized. Three scans were captured for Wide (12 mm × 9 mm), Macular Cube (7 mm × 7 mm–Triton; 6 mm × 6 mm–Maestro), and Optic Disc Cube (6 mm × 6 mm) scans for 25 normal eyes and 25 glaucoma eyes. Parameter measurements included circumpapillary retinal nerve fiber layer (cpRNFL), ganglion cell layer + inner plexiform layer (GCL+), and ganglion cell complex (GCL++). A two-way random effect analysis of variance model was used to estimate the repeatability and reproducibility; agreement was evaluated by Bland–Altman analysis and Deming regression. The precision estimates were low, indicating high precision, for all thickness measurements with the majority of the limits < 5 μm for the macula and < 10 μm for the optic disc. Precision of the Wide and Cube scans were comparable. Excellent agreement between the two devices was found for Wide scans, with the mean difference < 3 μm across all measurements (cpRNFL < 3 μm, GCL+ < 2 μm, GCL++ < 1 μm), indicating interoperability. A single Wide scan covering the peripapillary and macular regions may be useful for glaucoma diagnosis and management.

Primary open angle glaucoma (POAG) is characterized by progressive loss of retinal ganglion cells (RGCs) and their axons, and accompanying damage to the visual field (VF)¹ For most clinicians, management of glaucoma usually requires both a functional test, in particular, a VF obtained by automated perimetry, and a structural test, most commonly with optical coherence tomography (OCT) imaging². In addition to the useful OCT cross-sectional B scans, which allow for visualization of retinal structures, thickness measurements facilitate quantitative evaluation of the neural retina affected by glaucomatous damage. Thus, OCT is an irreplaceable imaging technology for glaucoma diagnosis and management.

Early detection and close monitoring of glaucomatous damage are important to avoid irreversible vision loss. Characteristic excavation and narrowing of the neuroretina rim of the optic disc as a result of nerve degeneration is the most well-known glaucomatous manifestation. Several studies have also suggested that glaucomatous damage to the macula, where more than 30% of the RGCs in the eye reside³, is common and can occur early in the disease^{4,5}. In addition, damage to the macular RGCs and peripapillary retinal nerve fiber layer (RNFL) likely follow certain patterns that are closely related with each other. Although a number of studies have found that measures of macular RGC and peripapillary RNFL thickness have similar sensitivity and specificity⁴, it is not expected for these measures to provide equivalent information. Therefore, clinicians need to be aware that measurements of both the peripapillary and macular regions are considered an indispensable part of the comprehensive evaluation of glaucomatous damage⁴.

¹Topcon Healthcare, 111 Bauer Dr, Oakland, NJ 07436, USA. ²Department of Ophthalmology, Hamilton Glaucoma Center, Shiley Eye Institute, University of California, San Diego, CA, USA. ✉email: hhou@topcon.com

Clinically available OCTs have various scan protocols for macular and optic disc measures. Typically, the macula and peripapillary regions are scanned independently to obtain the respective measures. However, it is useful to have methods for combining the information from both macular RGC and peripapillary RNFL measures in a single scan to aid clinical decision-making by recognizing patterns of glaucomatous damage⁴. Current generation OCTs allow wide field visualization of the retina with a scan area that encompasses both the macula and optic disc, making the clinical workflow for the technology more efficient and facilitating the investigation of macular and peripapillary OCT measurements simultaneously^{6–8}. Studies have shown that a wide field scan has glaucoma-discriminating ability comparable to a combination of more dense (macula and peripapillary) Cube scans^{6–8}. While the precision of macula and optic disc Cube scans has been well investigated^{9–12}, information on the repeatability and reproducibility of Wide scan measurements is limited. Moreover, even though both Swept-Source OCT (SS-OCT) and Spectral-Domain OCT (SD-OCT) technologies offer a Wide scan mode, no prior study has compared Wide scan measurements between these two devices. Considering that SD-OCT and SS-OCT devices are both abundantly accessible in eye care clinics and research environments, interoperability of their data would enhance clinical care and research¹³.

The purpose of this study was to evaluate the agreement of Wide scan measurements between Triton SS-OCT and Maestro SD-OCT and to assess the repeatability and reproducibility of measurements from the Wide scan and the Macula/Optic Disc Cube scans of the two devices in normal and glaucoma eyes, and to further evaluate the interoperability of these two technologies.

Methods

This was a prospective study. Subjects signed an informed consent form and fulfilled all inclusion and exclusion criteria. The IntegReview Institutional Review Board (3815 S. Capital of Texas Hwy, Suite 320, Austin, TX 78704) approved the study protocol, and the methodology adhered to the tenets of the Declaration of Helsinki for research involving human subjects and to the Health Insurance Portability and Accountability Act.

Participants

Subjects underwent an ocular examination to determine eligibility for study enrollment. Assessments included best-corrected visual acuity (BCVA), refraction, slit lamp biomicroscopy, ophthalmoscopy, intraocular pressure (IOP), and VF (standard automated perimetry, Humphrey Field Analyzer; 24–2 Swedish interactive threshold algorithm—standard; Carl Zeiss Meditec, Inc., Dublin, California).

Overall inclusion criteria for subjects in this study were 18 years of age or older on the date of informed consent, ability to understand the written informed consent, and willingness to participate as evidenced by signing the informed consent. All eligible subjects had a bilateral BCVA of 20/40 or better. Subjects were excluded if they were unable to tolerate ophthalmic imaging, had ocular media that precluded acceptable OCT images, history of leukemia, dementia or multiple sclerosis, or concomitant use of hydroxychloroquine or chloroquine. Subjects were excluded if their 24–2 VF result was unreliable (defined as fixation losses > 20%, false positives > 33%, or false negatives > 33%).

Subjects in the Normal group were defined as presenting with normal eyes bilaterally (non-visually impairing cataract was acceptable). Subjects had IOP ≤ 21 mmHg in each eye. Clinically defined normal subjects that had VF defects consistent with glaucomatous optic nerve damage based on at least one of the following findings or narrow angles in either eye were excluded from the Normal group: a) On pattern deviation (PD), there exists a cluster of 3 or more points in an expected location of the VF depressed below the 5% level, at least 1 of which is depressed below the 1% level; b) Glaucoma hemi-field test “outside normal limits”.

Subjects included in the Glaucoma group were defined as those with VF defects as described above consistent with glaucomatous optic nerve damage and having glaucomatous optic nerve damage as clinically evidenced by any of the following optic disc or RNFL structural abnormalities: a) Diffuse thinning, focal narrowing, or notching of the optic disc rim especially at the inferior or superior poles with or without disc hemorrhage; b) Localized abnormalities of the peripapillary RNFL, especially at the inferior or superior poles; c) Optic disc neural rim asymmetry of the two eyes consistent with loss of neural tissue.

Subjects were excluded from the Glaucoma group if they presented with presence of any ocular pathology except glaucoma in the study eye (non-visually impairing cataract was acceptable).

The study eye and the testing order of the operator/device configuration were randomized for each subject. If only one eye of a subject in the Glaucoma group had pathology and met the eligibility criteria, the eligible eye was the study eye. For eyes in the Normal group, both eyes were required to have met all normal eligibility criteria prior to study eye randomization.

Optical coherence tomography scans

This study included three SS-OCT devices (DRI OCT Triton, Topcon Inc, Tokyo, Japan) and three SD-OCT devices (3D OCT-1 Maestro, Topcon Inc, Tokyo, Japan). Three operators used these study devices to acquire the scans. Each operator was paired with one specific DRI OCT Triton and one specific 3D OCT-1 Maestro to create three distinct operator/device configurations. The OCT imaging was conducted during a single session. The scan types included for the Triton were Wide scan (12 mm × 9 mm), Optic Disc Cube (6 mm × 6 mm), and Macular Cube (7 mm × 7 mm) scans. The scan types included for the Maestro were Wide scan (12 mm × 9 mm), Optic Disc Cube (6 mm × 6 mm), and Macular Cube (6 mm × 6 mm) scans. Figure 1 shows representative OCT reports of these scan types from Maestro and Triton. Circumpapillary RNFL (cpRNFL) thickness measurements were derived from the Wide and Optic Disc Cube scans. Macula ganglion cell layer (GCL) and inner plexiform layer (IPL) (mGCIPL, abbreviated on the instrument reports and in this study to mGCL+) thickness and macula ganglion cell complex (mGCC, abbreviated on the instrument reports and in this study to mGCL++) thickness

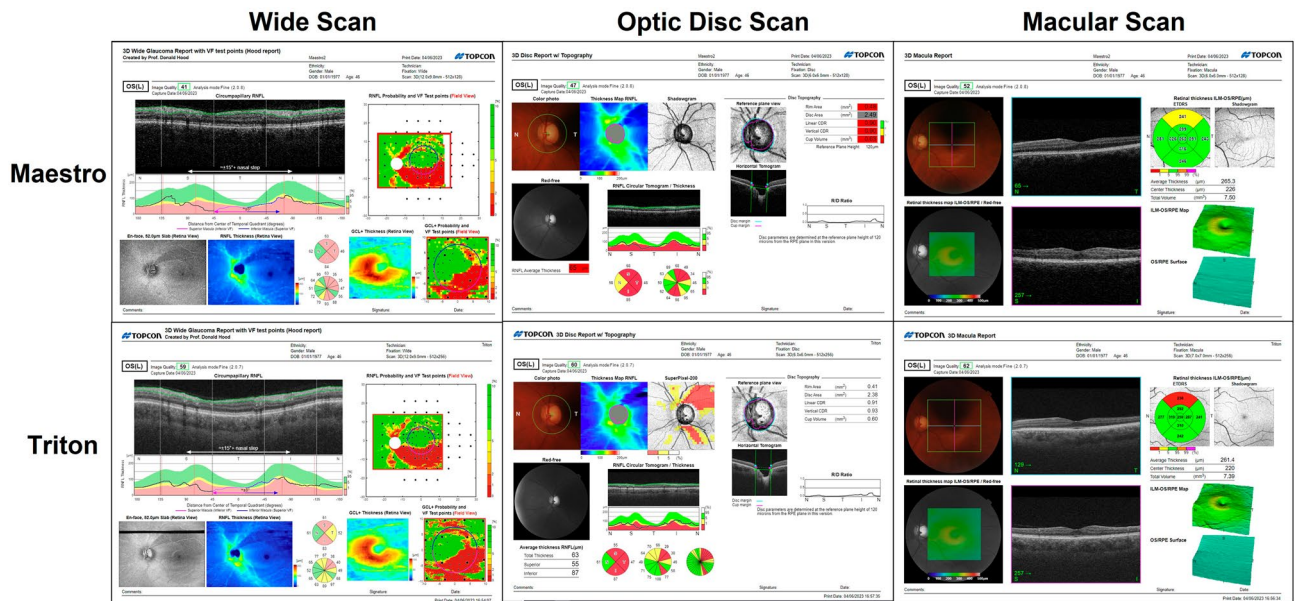


Figure 1. Representative OCT reports of Wide scan and Cube scans from one glaucoma eye (24–2 visual field mean deviation -3.56 dB). The top row shows the reports of (left to right) Wide scan (12 mm × 9 mm), Optic Disc Cube scan (6 mm × 6 mm), and Macular Cube scan (6 mm × 6 mm) from the Maestro; and the bottom row shows the reports of (left to right) Wide scan (12 mm × 9 mm), Optic Disc Cube scan (6 mm × 6 mm), and Macular Cube scan (7 mm × 7 mm) from the Triton.

were derived from the Wide and Macular Cube scans. For each scan type, at least 3 scans per eye for each operator/device configuration were taken.

All scans of each study subject were evaluated by two independent masked imaging experts in a randomized fashion for image quality acceptance. The graders were blinded to operator, device, subject ID, subject data, and each other’s grading. Individual B scan evaluation was conducted on the central horizontal B scan from the first of the three volume scans captured from each scan type (Wide, Macular Cube, Optic Disc Cube). Key aspects of a scan to consider for acceptable image quality were: 1. overall signal strength, 2. local weak signal, 3. poor centration of key structures (fovea not in center of macula scans), 4. eye movements, 5. clipping of the retina (scan too high or too low or full retina chopped off), 6. segmentation failure, and 7. improper placement of the macula grid. Acceptable quality scans passed each of these image quality tests. Any scan deemed unacceptable was not included in the data analysis.

Statistical analysis

In general, descriptive statistics (n, mean, standard deviation (SD), and median) were used to summarize continuous variables. Frequencies and percentages were used to summarize categorical variables.

The precision analysis was conducted utilizing all acceptable scans for both the Triton SS-OCT and Maestro SD-OCT for all scan types. A two-way random effect analysis of variance (ANOVA) model was used to estimate the repeatability and reproducibility of each scan parameter by group and study device (Triton and Maestro). This ANOVA model included the operator/device, eye, and interaction between operator/device and eye as the variance components. The repeatability and reproducibility limits and coefficient of variation in percentage (CV%) were produced for each scan parameter by group and device. Specifically, repeatability SD = square root of the residual variance; reproducibility SD = square root of the sum of the operator/device variance, the interaction variance, and the residual variance; repeatability limit = $2.8 \times$ repeatability SD; reproducibility limit = $2.8 \times$ reproducibility SD; repeatability CV% = (repeatability SD)/intercept \times 100%; reproducibility CV% = (reproducibility SD)/intercept \times 100%.

Analysis of agreement included the first acceptable scan from each scan type (Wide scan, Macular Cube scan, and Optic Disc Cube scan) from the Triton and Maestro. Agreement between the two devices was evaluated using Bland–Altman plots to calculate the mean difference and the limits of agreement (LOA), and Deming regression to calculate slope (proportional bias) and intercept (systematic bias or offset), for each scan type in each group. Deming regression is similar to linear regression but accounts for variance in both variables. It is useful to estimate bias between methods in comparison studies such as the current one.

The sample size was determined based on the 95% LOA and the two-way random effect ANOVA model for precision. A sample size of 21 eyes per population was deemed sufficient to obtain at least 90% power at a one-sided significance level of 5% using an F-test to detect a variance of operator/device effect that was 50% of the total variance.

Statistical analyses were performed using statistical software SAS 9.3 or later (SAS Institute, Cary, North Carolina). P values less than 0.05 were considered statistically significant.

Results

Eight subjects (2 normal subjects and 6 glaucoma subjects) did not have acceptable scans from the Triton or Maestro and were excluded. 25 Normal subjects (25 eyes) and 25 Glaucoma subjects (25 eyes) were included. Demographic and ocular parameters of the study subjects are summarized in Table 1. The mean overall age was 59.3 ± 16.8 years, with the Glaucoma group being older. The study population was almost equally distributed between genders (52% male and 48% female). Most study eyes (78%) had a BCVA of 20/20 or better. For eyes in the Glaucoma group, the mean 24–2 mean deviation (MD) was -5.30 ± 6.77 dB and the mean pattern standard deviation (PSD) was 4.70 ± 2.87 dB. Among eligible subjects, scan rejection rates ranged up to 20% in the Wide scans and up to 11% in the Disc and Macula Cube scans across devices. Top reasons for scan rejection across all scan types included low signal strength, eye movement and segmentation failure.

Precision including repeatability and reproducibility of measurements from Wide and Cube scans was evaluated and compared. Overall, the precision estimates (reproducibility limit, reproducibility CV%, repeatability limit and repeatability CV%) were low, indicating high precision for all measurements (cpRNFL, GCL+, and GCL++ thickness). Precisions of the Wide and Cube scans were mostly similar in each device.

Table 2 summarizes the repeatability and reproducibility estimates of GCL+ thickness measurements in Normal and Glaucoma groups. In the Normal group, the CV% for repeatability and reproducibility of both Triton and Maestro OCT devices ranged between 0 and 1% with the exception of the reproducibility CV% for inferior thickness from the Maestro Wide scan, which was 1.1%. The CV% were generally higher in the Glaucoma group with a range of repeatability CV% between 0.6 to 1.7% for the Triton Wide scan and 0.5 to 1.4% for the Triton Macular Cube scan.

Supplement Table 1 summarizes the repeatability and reproducibility estimates of GCL++ thickness measurements in the Normal and Glaucoma groups. GCL++ thickness measurements from both scan types in the two devices showed excellent precision in the Normal and Glaucoma groups with CV% of repeatability and reproducibility within 1%, with the exception of CV% of reproducibility on the Maestro for the Superior Nasal region in the Glaucoma group, which was 1.1%. The repeatability limit of the Wide scan ranged from 1.1 to 2.1 μm for the Triton and from 1.2 to 2.1 μm for the Maestro. The reproducibility limit of the Wide scan ranged from 1.6 to 2.4 μm for the Triton and from 1.4 to 2.9 μm for the Maestro in both groups.

	Normal	Glaucoma
By subject (No.)	25	25
Age (years)		
Mean \pm SD / Median	42.7 \pm 14.7 / 40.0	67.6 \pm 10.4 / 68.0
Min/Max	21 / 75	44 / 85
Age group, no. (%)		
< 65 years	24 (96)	10 (40)
\geq 65 years	1 (4)	15 (60)
Gender (M/F)	14/11	12/13
Race, Caucasian, no. (%)	25 (100)	25 (100)
By Eye (No.)	25	25
BCVA, no. (%)		
20/20 or better	24 (96)	15 (60)
20/21–20/40	1 (4)	10 (40)
MRSE (D)		
Mean \pm SD	- 0.70 \pm 1.61	- 1.07 \pm 1.83
Min/Max	- 5.13 / 1.88	- 7.25 / 1.75
Axial length (mm)		
Mean \pm SD / Median	23.93 \pm 1.08 / 23.72	24.81 \pm 1.28 / 24.86
Min/Max	22.01 / 27.28	22.10 / 26.74
IOP (mmHg)		
Mean \pm SD / Median	15.2 \pm 3.1 / 16.0	14.4 \pm 2.8 / 15.0
Min/Max	8 / 20	8 / 19
24–2 Visual field MD (dB)		
Mean \pm SD	N/A	- 5.30 \pm 6.77
Min/Max		- 26.8 / - 0.6
24–2 Visual field PSD (dB)		
Mean \pm SD	N/A	4.70 \pm 2.87
Min/Max		1.9 / 12.9

Table 1. Demographics and ocular characteristics of study groups. *SD*, standard deviation; *Min*, minimum; *Max*, maximum; *BCVA*, best corrected visual acuity; *D*, diopter; *MRSE*, manifest refraction spherical equivalent; *IOP*, intraocular pressure; *MD*, mean deviation; *PSD*, pattern standard deviation.

	Triton 12×9 mm ² Wide Scan			Triton 7×7 mm ² Macular Scan			Maestro 12×9 mm ² Wide Scan			Maestro 6×6 mm ² Macular Scan		
	SD	Limit	CV%	SD	Limit	CV%	SD	Limit	CV%	SD	Limit	CV%
Repeatability												
Normal group												
Average	0.3	0.7	0.4	0.2	0.6	0.3	0.2	0.6	0.3	0.3	0.7	0.3
Superior	0.5	1.5	0.8	0.4	1.2	0.6	0.6	1.8	0.9	0.5	1.5	0.7
Superior Nasal	0.4	1.1	0.5	0.4	1.1	0.5	0.5	1.4	0.7	0.5	1.3	0.6
Superior Temporal	0.5	1.4	0.7	0.6	1.7	0.8	0.5	1.4	0.7	0.6	1.6	0.8
Inferior	0.4	1.1	0.6	0.5	1.3	0.7	0.6	1.6	0.8	0.5	1.4	0.7
Inferior Nasal	0.4	1.0	0.5	0.5	1.3	0.6	0.6	1.6	0.8	0.4	1.2	0.6
Inferior Temporal	0.5	1.4	0.7	0.7	1.8	0.9	0.5	1.5	0.7	0.5	1.4	0.7
Glaucoma group												
Average	0.4	1.0	0.6	0.3	0.8	0.5	0.8	2.2	1.3	0.4	1.0	0.6
Superior	0.9	2.5	1.6	0.5	1.4	0.9	1.1	3.2	2.0	0.6	1.7	1.1
Superior Nasal	0.5	1.3	0.7	0.4	1.2	0.7	0.7	1.9	1.1	0.4	1.2	0.7
Superior Temporal	0.8	2.1	1.3	0.8	2.3	1.4	1.3	3.7	2.3	0.7	2.1	1.2
Inferior	0.6	1.7	1.1	0.5	1.5	1.0	1.0	2.7	1.8	0.8	2.3	1.5
Inferior Nasal	0.6	1.6	1.0	0.6	1.8	1.1	0.9	2.6	1.6	0.7	2.0	1.2
Inferior Temporal	0.9	2.6	1.7	0.8	2.3	1.4	2.1	6.0	3.8	0.7	2.0	1.2
Reproducibility												
Normal group												
Average	0.3	1.0	0.5	0.4	1.1	0.5	0.3	0.9	0.5	0.4	1.1	0.5
Superior	0.7	1.9	1.0	0.6	1.7	0.9	0.7	2.0	1.0	0.6	1.7	0.8
Superior Nasal	0.5	1.4	0.7	0.5	1.4	0.7	0.6	1.7	0.8	0.5	1.5	0.7
Superior Temporal	0.6	1.7	0.8	0.7	2.0	1.0	0.6	1.7	0.8	0.6	1.7	0.9
Inferior	0.5	1.3	0.7	0.6	1.7	0.9	0.8	2.1	1.1	0.7	2.0	1.0
Inferior Nasal	0.4	1.2	0.6	0.6	1.7	0.8	0.7	1.9	0.9	0.6	1.6	0.8
Inferior Temporal	0.6	1.6	0.8	0.8	2.1	1.0	0.6	1.7	0.8	0.6	1.8	0.8
Glaucoma group												
Average	0.5	1.3	0.8	0.4	1.2	0.7	0.9	2.5	1.5	0.4	1.2	0.7
Superior	1.0	2.8	1.8	0.7	1.8	1.2	1.3	3.7	2.3	0.7	1.8	1.1
Superior Nasal	0.5	1.5	0.9	0.5	1.4	0.8	0.7	2.0	1.2	0.5	1.5	0.9
Superior Temporal	0.9	2.4	1.5	0.9	2.4	1.4	1.5	4.1	2.5	0.8	2.2	1.3
Inferior	0.7	1.8	1.2	0.7	2.0	1.3	1.1	3.1	2.0	0.9	2.5	1.6
Inferior Nasal	0.6	1.8	1.1	0.8	2.1	1.3	0.9	2.6	1.6	0.8	2.2	1.3
Inferior Temporal	1.1	3.1	2.0	1.0	2.8	1.7	2.4	6.8	4.3	0.9	2.5	1.5

Table 2. Repeatability and reproducibility of ganglion cell and internal plexiform layer thickness measurements. Unit of SD and limit is μm . Abbreviations: SD, standard deviation.

Table 3 shows the repeatability and reproducibility estimates of RNFL thickness measurements in the Normal and Glaucoma groups. Overall, precision of RNFL thickness was inferior to that of macular measurements in both the Normal and Glaucoma groups. The CV% for repeatability and reproducibility of the Triton Wide scan measures in glaucoma eyes ranged between 1.4–2.9% and 1.6–3.4% respectively, similar with the Optic Disc Cube scan (1.3–2.9% and 1.7–3.2%, respectively). All the limit estimates for the Triton were $< 10 \mu\text{m}$ in both groups; repeatability and reproducibility limits of Wide scan measurements for glaucoma eyes ranged between 3.0–6.5 μm and 3.4–7.2 μm , respectively). In comparison, the Maestro showed slightly higher limit estimates (maximum 11.8 μm).

Assessment of Wide scan macular and peripapillary RNFL thickness agreement showed that the measurement differences between the Triton and Maestro were small across all parameters. Supplement Tables 2 and 3 summarized agreements of GCL+, GCL++, and cpRNFL thickness measurements from the Wide scan between Triton and Maestro. The mean differences of GCL+ thickness and GCL++ thickness between the two devices were $< 2 \mu\text{m}$ and $< 1 \mu\text{m}$, respectively, in both groups. For GCL+ thickness measurements, Triton had slightly lower measurements than Maestro in both groups. GCL++ thickness measurements were slightly higher for Triton in the Glaucoma group, but more comparable in the Normal Group. From Supplement Table 3, RNFL thickness measurements were slightly higher for Triton in the Glaucoma group (mean difference between the two devices $< 3 \mu\text{m}$), and slightly lower in the Normal group except for nasal sector. All the differences were very minimal and not statistically significant.

Deming regression showed that all the slopes for the Triton and Maestro were close to +1, and most of the 95% confidence intervals (CIs) for the intercept and slope contained 0 and 1, respectively, that is, the intercepts

	Triton 12×9 mm ² Wide Scan			Triton 6×6 mm ² Optic Disc Scan			Maestro 12×9 mm ² Wide Scan			Maestro 6×6 mm ² Optic Disc Scan		
	SD	Limit	CV%	SD	Limit	CV%	SD	Limit	CV%	SD	Limit	CV%
Repeatability												
Normal group												
Average	0.9	2.6	0.9	0.8	2.1	0.7	1.3	3.7	1.2	0.8	2.2	0.8
Superior	2.9	8.2	2.3	2.1	6.0	1.6	3.9	11.0	3.0	2.5	7.1	1.9
Nasal	1.7	4.8	1.9	1.4	3.9	1.6	2.0	5.7	2.3	1.5	4.1	1.7
Inferior	2.2	6.3	1.6	1.4	4.0	1.0	2.7	7.6	1.9	2.1	5.8	1.5
Temporal	1.0	2.9	1.4	0.8	2.2	1.1	1.2	3.3	1.7	1.1	3.0	1.5
Glaucoma group												
Average	1.1	3.0	1.4	1.0	2.8	1.3	1.5	4.1	1.9	1.2	3.4	1.6
Superior	2.3	6.4	2.6	2.6	7.2	2.9	3.4	9.6	4.0	2.4	6.8	2.8
Nasal	1.8	5.1	2.9	1.7	4.7	2.7	3.1	8.7	5.1	2.5	6.9	4.1
Inferior	2.3	6.5	2.5	1.9	5.2	2.0	3.0	8.3	3.3	2.7	7.6	3.0
Temporal	1.1	3.0	1.7	0.9	2.5	1.5	1.2	3.4	2.0	1.4	3.9	2.4
Reproducibility												
Normal group												
Average	1.1	3.1	1.0	1.0	2.9	1.0	1.4	3.9	1.3	1.0	2.9	1.0
Superior	3.1	8.7	2.4	2.4	6.6	1.8	4.2	11.8	3.2	2.6	7.2	2.0
Nasal	2.1	6.0	2.4	1.7	4.8	2.0	2.3	6.4	2.6	1.8	5.0	2.1
Inferior	2.3	6.5	1.7	1.8	5.0	1.3	3.1	8.6	2.2	2.4	6.6	1.7
Temporal	1.4	3.9	2.0	1.1	3.0	1.6	1.3	3.7	1.8	1.3	3.7	1.9
Glaucoma group												
Average	1.2	3.4	1.6	1.3	3.5	1.7	1.7	4.8	2.3	1.3	3.7	1.8
Superior	2.6	7.2	2.9	2.8	7.9	3.2	3.6	10.1	4.2	2.6	7.2	3.0
Nasal	2.2	6.1	3.4	1.9	5.4	3.2	3.7	10.2	6.0	2.9	8.2	4.9
Inferior	2.5	7.0	2.7	2.1	5.9	2.3	3.3	9.1	3.6	2.7	7.6	3.0
Temporal	1.3	3.6	2.1	1.1	3.0	1.8	1.3	3.7	2.2	1.5	4.2	2.6

Table 3. Repeatability and reproducibility of retinal nerve fiber layer thickness measurements. Unit of SD and limit is μm . Abbreviations: SD, standard deviation.

did not significantly differ from 0 and slopes did not differ significantly from 1, indicating excellent agreement of the Wide scan measurements between Triton and Maestro. Representative Bland–Altman plots and Deming regression plots are shown in Figs. 2, 3, and Supplement Fig. 1, which illustrate agreement of GCL+, cpRNFL, and GCL++ thickness measurements from the Wide scan between Triton and Maestro in the Glaucoma group, respectively.

Discussion

This study demonstrated that Wide scan measurements from the Triton SS-OCT and Maestro SD-OCT have excellent agreement in both normal and glaucoma eyes. In addition, the repeatability and reproducibility of cpRNFL, macular GCL+, and macular GCL++ thickness measurements from the Wide and the Macular/ Optic Disc Cube scans were similar for both the Triton and the Maestro in normal and glaucoma eyes.

Measuring structural changes is essential for diagnosing and monitoring glaucoma¹, and OCT is a well-established method to objectively assess structural changes in eyes with glaucoma¹⁴. Before the introduction of a Wide scan that simultaneously captures peripapillary and macular anatomical structures in one scan, separate Macular and Optic Disc Cube scans were required to quantitatively assess macular RGCs and RNFL respectively. However, in clinical practice, often only one OCT scan, typically the Optic Disc Cube scan, is captured due to time limitations⁷. Rather than acquiring data with both Macular and Optic Disc Cube scans, the Wide scan and its incorporated automated segmentation software makes it possible to analyze the thickness of peripapillary RNFL and various macular retinal layers simultaneously using data obtained with only a single scan. As found in the current study, the Wide scan and Cube scan measurements are comparable. Moreover, imaging time is reduced with simultaneous imaging of the macula and the peripapillary region relative to the capturing of two scans per eye. This also minimizes the adverse impact on image quality caused by patient fatigue, motion, and alignment errors. In addition, the paracentral fixation target of the Wide scan reduces the fixation errors caused during acquisition of the Optic Disc Cube scan which requires nasal fixation^{8,15}. Another strength of the Wide scan is that peripapillary RNFL defects at 11 and 12 o'clock (in the right eye orientation) can be missed in the Macular Cube scans, while they are more likely visualized in a Wide scan including both cpRNFL and macular GCC¹⁶. Another study has shown that the thickness map provided for Wide scans detects early structural changes that

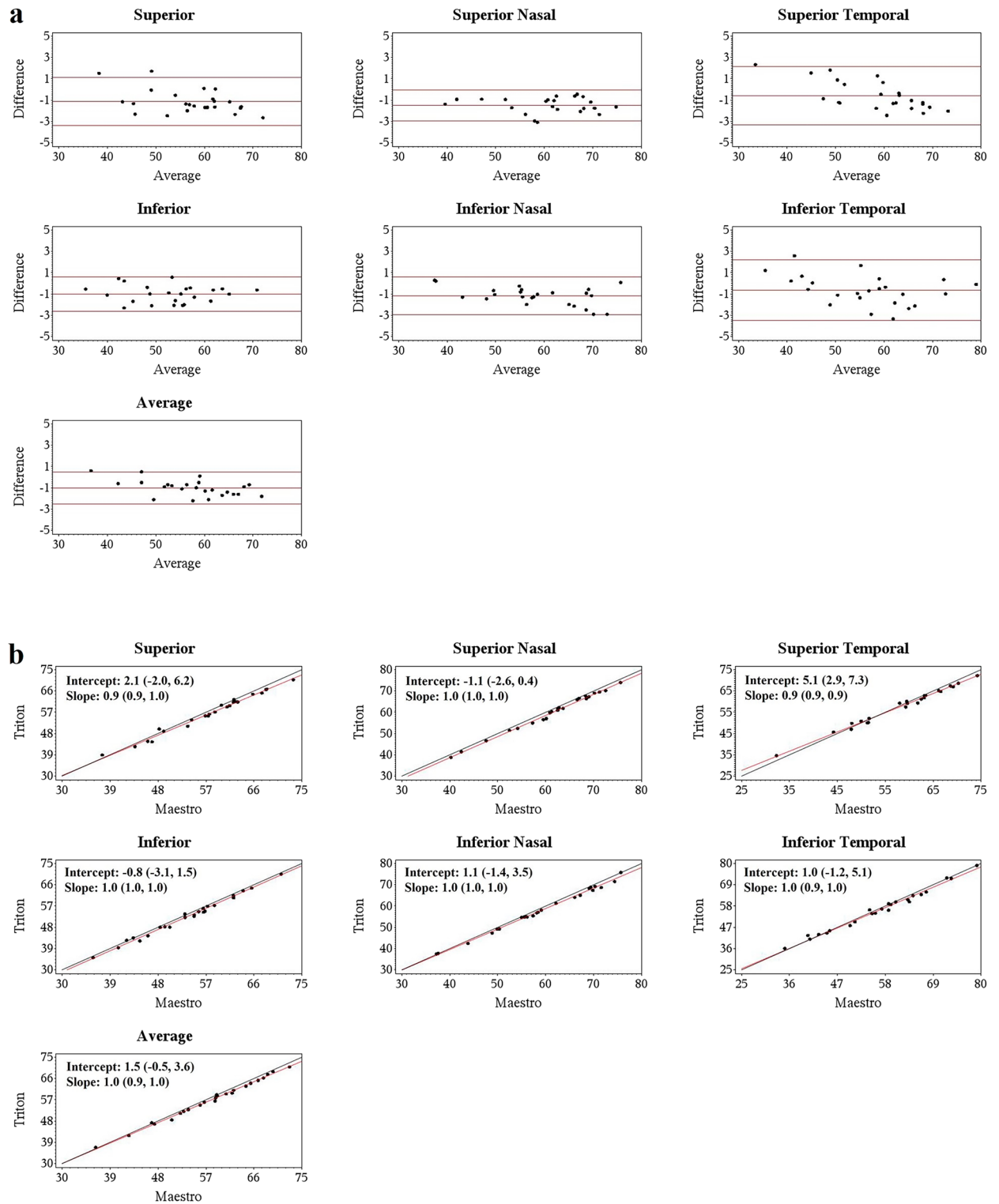


Figure 2. Agreement assessment of Wide scan ganglion cell layer and inner plexiform layer (GCL+) thickness between the Triton and Maestro in glaucoma eyes. **(a)** Bland–Altman plots showing mean differences of Wide scan GCL+ thickness between the Triton and Maestro in glaucoma eyes were less than 2 μm . **(b)** Deming regression plot of thickness of GCL+ from the Wide scan of Triton and Maestro in glaucoma eyes. The plots illustrate the fitted linear models (red line) and the identity lines (Triton measurement = Maestro measurement, slope = 1) (black line). Intercepts and slopes of the fitted linear model are shown as mean (95% confidence interval) and indicate excellent agreement of the Wide scan measurements between Triton and Maestro.

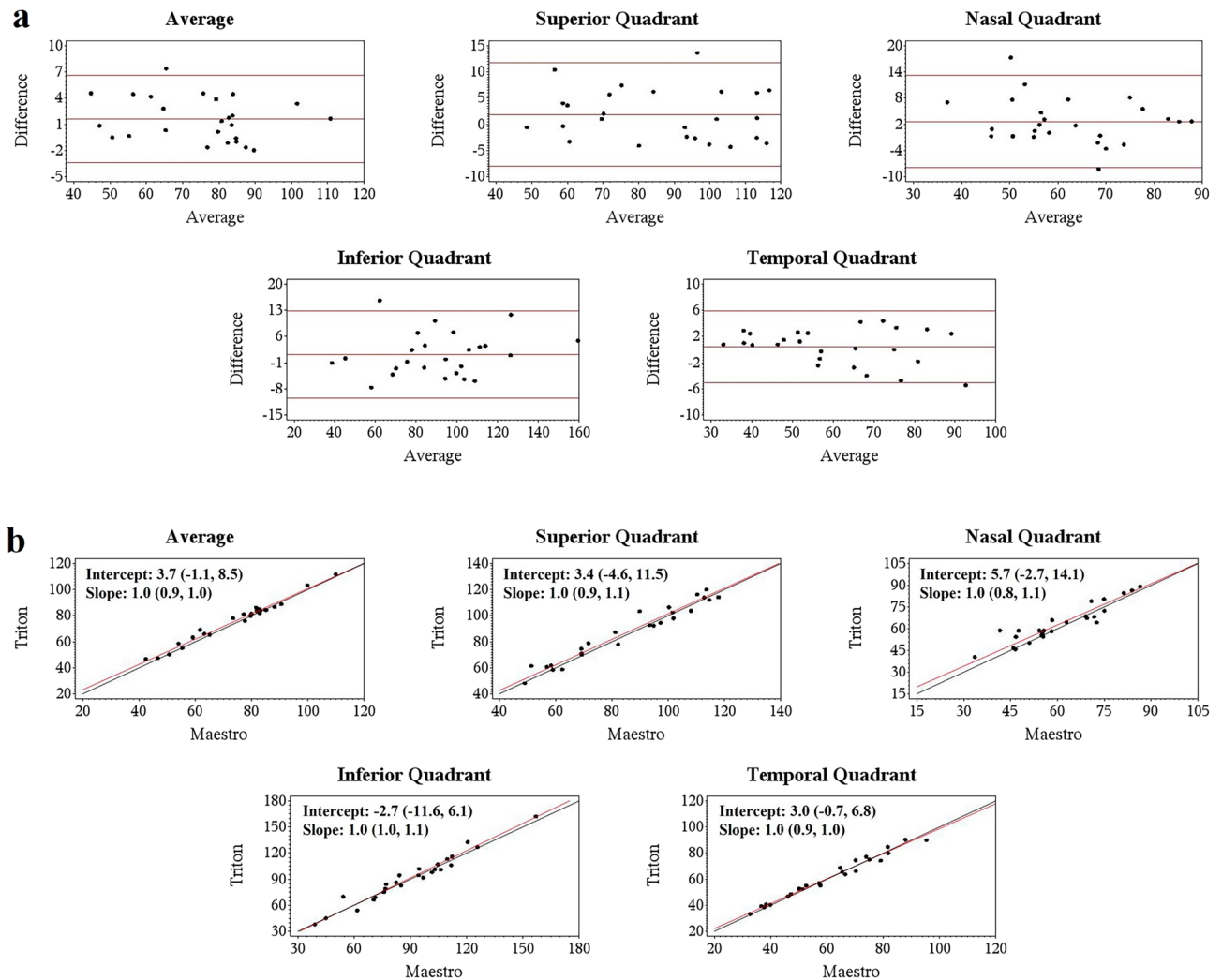


Figure 3. Agreement assessment of Wide scan circumpapillary retinal nerve fiber layer (cpRNFL) thickness between the Triton and Maestro in glaucoma eyes. **(a)** Bland–Altman plots showing mean differences of Wide scan cpRNFL thickness between the Triton and Maestro in glaucoma eyes were less than 3 μm . **(b)** Deming regression plot of thickness measurements of cpRNFL from the Wide scan between Triton and Maestro in glaucoma eyes. The plots illustrate the fitted linear models (red line) and the identity lines (Triton measurement = Maestro measurement, slope = 1) (black line). Intercepts and slopes of the fitted linear models, which are shown as mean (95% confidence interval), indicate measurements of the two devices were in excellent agreement.

might not be detected well using peripapillary RNFL or macular GCIPL thickness maps. Furthermore, RNFL defects distant from the optic disc can be more easily visualized with the Wide scan RNFL maps¹⁷.

The diagnostic power of the Wide scan has been evaluated by several studies. Yang et al.¹⁸ compared the diagnostic ability (healthy vs glaucoma) of RNFL¹⁸ and macular GCIPL and macular GCC¹⁹ thickness values from a SS-OCT Wide scan (DRI-OCT, Topcon) and Macular/Optic Disc Cube scans of a SD-OCT (Spectralis, Heidelberg Engineering and Cirrus HD-OCT, Carl Zeiss Meditec), and reported that RNFL, macular GCIPL, and macular GCC thickness values from the Wide scan measured by SS-OCT had similar diagnostic accuracy to Macular/Optic Disc Cube scan measurements obtained by SD-OCT. Similarly, another study showed the diagnostic ability of SS-OCT (DRI-OCT-1 Atlantis, Topcon) Wide scan measurements for distinguishing pre-perimetric and early glaucoma from healthy eyes was similar to Macular/Optic Disc Cube scan measurements from SD-OCT (Cirrus HD-OCT, Carl Zeiss Meditec)⁶. These previous studies compared diagnostic ability of SS-OCT Wide scan with SD-OCT Cube scan, while Hong et al.⁸ compared glaucoma-discriminating ability of measurements from Wide scans with Macular/Optic Disc Cube scans of SS-OCT (DRI-OCT-1 Atlantis, Topcon) and reported that they were comparable. Furthermore, Hood et al.⁷ reported that the report based upon a single Wide scan has the information needed to diagnose early glaucoma with excellent sensitivity and specificity. Thus, it has been suggested that the Wide scan could replace Macular/Optic Disc Cube scans for diagnosing and screening glaucoma^{7,8}.

Besides discrimination between normal and glaucoma, monitoring patients with glaucoma to detect progression is the mainstay of glaucoma care, which requires reliable measures with good repeatability and

reproducibility²⁰. Studies addressing measurement precision of Wide scans are limited. One study¹⁵ using SD-OCT (Canon OCT-HS100, Canon Europe) compared repeatability of measurements from a Wide scan (13 mm × 10 mm) and Cube scans (Macular scan 10 mm × 10 mm, Optic Disc scan 6 mm × 6 mm) in healthy eyes. Different from our results, they found a 2–3 times larger repeatability limit of the Wide scan compared with the Cube scans. The authors attributed their result partially to the scan density in the Wide scan, which is 4.4 times less than for the individual Cube scans. By contrast, the Wide scan and Cube scan in the current study are closer in scan density. It has also been reported previously that the scan direction affects precision, where horizontal scans have better repeatability than vertical scans²¹. The Wide scan in the prior study employed vertical B-scans, while the Optic Disc and Macular Cube scans were captured horizontally and vertically, respectively¹⁵, thereby potentially contributing to the varied repeatability between the Wide and Cube scans. With SS-OCT (DRI-OCT-1 Atlantis, Topcon), another study⁸, found comparably good repeatability of macular GCIPL and macular GCC thickness values from the Wide scan and Cube scans in healthy and glaucoma eyes; the current results are consistent with these earlier ones. The current study expands on that earlier one as it evaluated repeatability and reproducibility in normal and glaucoma eyes. It shows comparable precision of parameters relevant for glaucoma management between the Wide scan and Macular and Optic Disc Cube scans for both the Triton and Maestro OCT devices.

Agreement between SS-OCT and SD-OCT, as well as agreement between the Wide scan and Macular/ Optic Disc Cube scans have been previously studied. Lee SY et al.²² evaluated agreement between SS-OCT and SD-OCT Cube scans, and Lee WJ et al.⁶ evaluated agreement between SS-OCT Wide scan and SD-OCT Cube scans, respectively, in normal eyes using the same devices (SS-OCT: DRI-OCT-1 Atlantis, Topcon vs. SD-OCT: Cirrus HD-OCT, Carl Zeiss Meditec); while Yang et al.¹⁹ evaluated agreement between SS-OCT Wide scan (DRI-OCT, Topcon) and SD-OCT Cube scans (Cirrus HD-OCT, Carl Zeiss Meditec) for healthy and glaucomatous eyes. In all of these studies, the comparison included different manufacturers, algorithms, and measurement positions and grids. In contrast, the Triton and Maestro share segmentation algorithms and measurement locations. That may explain why the differences observed in this study were generally smaller than those in previous studies. Importantly, the differences between Triton and Maestro (mean difference of all measurements < 3 μm) were less than the axial resolution in tissue (Triton axial resolution 8 μm, Maestro axial resolution 6 μm²³), and smaller than the corresponding reproducibility limits. Therefore, these differences are assumed not to be clinically significant. However, as shown in the Supplement Table 2, some of the 95% CIs for the upper LOA of GCL+ thickness of glaucoma eyes were not statistically different from zero, indicating there may be small but systematic difference between the two devices. Hence, the clinician may want to use caution including data from both devices in a progression analysis for this specific set of parameters. While for GCL++ and cpRNFL thickness (Supplement Tables 2 and 3), the 95% CIs included zero and any differences were negligible. Thus, GCL++ and cpRNFL thickness may be preferred in progression analysis. The reported agreement results were expected based on minor differences in axial resolution, software and algorithm, and a minimal difference in the pixel calibration factor between Triton and Maestro. In addition, Hong et al.⁸ found excellent agreement for macular GCIPL, macular GCC and peripapillary RNFL measurements between the SS-OCT (DRI-OCT-1 Atlantis, Topcon) Wide scan and Cube scans for healthy and glaucomatous eyes; Dominguez-Vicent et al.¹⁵ showed that measurement differences between the Wide and Cube scans for SD-OCT (Canon OCT-HS100, Canon Europe) were mostly lower than the axial resolution of the device for healthy eyes. In summary, these studies suggested that, for glaucoma follow up, consistency of scan type, device, and OCT technology need to be considered. Although the same device and scan type is optimal, this study demonstrates that measurement interchangeability may be expected within certain configurations of parameters, scan types and devices, such as GCL++ and cpRNFL thickness from the 12 mm × 9 mm Wide scan of the Triton SS-OCT and the Maestro SD-OCT.

There are several limitations of this study. First, the results of this study were obtained entirely from Caucasian subjects. Although we do not expect ethnicity to directly affect repeatability or reproducibility, additional studies using subjects from different populations would generalize our conclusions. Second, there was a significant difference in age distributions between Normal and Glaucoma groups. The influence of the inter-group age difference on the current study results (from inter-scan type and inter-device analyses) is negligible because all estimates were presented for each single group without inter-group comparison. The range of retinal thickness measurements of normal subjects from this study were highly similar with that in other publications^{24–26}. Moreover, although the retinal thickness measurements decrease with age (total retina thinning 0.53 μm/year; RNFL thinning 0.44 μm/year²⁷), there is no evidence that the rate of age-related thinning varies in different age groups. Therefore, even if test interval is long enough to affect the evaluation of repeatability and reproducibility, which is not applicable for the current study, the effect should be equal between the groups. Nevertheless, one should take the applicable age range into consideration when interpreting the values of retinal thickness of each group. Third, the glaucoma patients included in this study had an average MD of -5.30 dB indicating that most subjects had early to moderate glaucoma. Studies with a wider distribution of glaucoma severity are needed to evaluate the utility of the Wide scan in advanced disease. Fourth, the sample size of the current study is relatively small with 25 eyes in each group. The sample size was determined based on the 95% LOA and the ANOVA model for precision and 21 eyes per group were deemed appropriate. Lastly, although this study suggests a potential role of a Wide scan for glaucoma monitoring, this cross-sectional study was unable to evaluate how well the Wide scan measurements of Triton and Maestro can identify glaucomatous progression. Longitudinal studies are needed to further evaluate the clinical utility of Wide scans in monitoring glaucoma progression.

In conclusion, we have demonstrated high and comparable precision of peripapillary and macula thickness measurements from Wide, Macular Cube, and Optic Disc Cube scans of the Triton SS-OCT and the Maestro SD-OCT in normal and glaucoma eyes. Wide scan measurements of the Triton SS-OCT and Maestro SD-OCT were interchangeable with excellent agreement. These findings show the potential for more simultaneous evaluation

of both macular and peripapillary retinal anatomy from a single Wide OCT scan rather than the clinical standard of capturing an Optic Disc Cube scan and a Macular Cube scan for glaucoma diagnosis and management.

Data availability

The datasets used and/or analysed during the current study available from the corresponding author on reasonable request.

Received: 31 May 2023; Accepted: 21 September 2023

Published online: 23 September 2023

References

- Weinreb, R. N., Aung, T. & Medeiros, F. A. The pathophysiology and treatment of glaucoma: A review. *JAMA* **311**, 1901 (2014).
- Hood, D. C. *et al.* Detecting glaucoma with only OCT: Implications for the clinic, research, screening, and AI development. *Prog. Retin. Eye Res.* **90**, 101052 (2022).
- Curcio, C. A. & Allen, K. A. Topography of ganglion cells in human retina. *J. Comp. Neurol.* **300**, 5–25 (1990).
- Hood, D. C. *et al.* Glaucomatous damage of the macula. *Prog. Retin. Eye Res.* **32**, 1–21 (2013).
- Traynis, I. *et al.* Prevalence and nature of early glaucomatous defects in the central 10° of the visual field. *JAMA Ophthalmol.* **132**, 291 (2014).
- Lee, W. J. *et al.* Comparison of glaucoma-diagnostic ability between wide-field swept-source OCT retinal nerve fiber layer maps and spectral-domain OCT. *Eye* **32**, 1483–1492 (2018).
- Hood, D. C. *et al.* A single wide-field OCT protocol can provide compelling information for the diagnosis of early glaucoma. *Trans. Vis. Sci. Tech.* **5**, 4 (2016).
- Hong, E. H. *et al.* Wide scan imaging with swept-source optical coherent tomography for glaucoma diagnosis Vavvas DG, ed. *PLoS ONE* **13**, e0195040 (2018).
- Matlach, J., Wagner, M., Malzahn, U. & Göbel, W. Repeatability of Peripapillary retinal nerve Fiber layer and inner retinal thickness among two spectral domain optical coherence tomography devices. *Invest. Ophthalmol. Vis. Sci.* **55**, 6536 (2014).
- Ctori, I. & Huntjens, B. Repeatability of foveal measurements using spectralis optical coherence tomography segmentation software stieger K, ed. *PLoS ONE* **10**, e0129005 (2015).
- Savini, G., Carbonelli, M., Parisi, V. & Barboni, P. Repeatability of optic nerve head parameters measured by spectral-domain OCT in healthy eyes. *Ophthalmic Surg. Lasers Imag.* **42**, 209–215 (2011).
- Brautaset, R. *et al.* Repeatability using automatic tracing with canon OCT- HS100 and Zeiss cirrus HD-OCT 5000 Rubin DL, ed. *PLoS ONE* **11**, e0149138 (2016).
- Mun, Y. *et al.* An innovative strategy for standardized, structured, and interoperable results in ophthalmic examinations. *BMC Med. Inform. Decis. Mak.* **21**, 9 (2021).
- Leung, C. K. S. Diagnosing glaucoma progression with optical coherence tomography. *Curr. Opin. Ophthalmol.* **25**, 104–111 (2014).
- Dominguez-Vicent, A. *et al.* Precision and agreement of individual and simultaneous macular and optic disc volumetric measurements with spectral domain optical coherence tomography. *Front Med* **8**, 764236 (2021).
- Kim, K. E. *et al.* Topographic localization of macular retinal ganglion cell loss associated with localized Peripapillary retinal nerve Fiber layer defect. *Invest. Ophthalmol. Vis. Sci.* **55**, 3501 (2014).
- Lee, W. J. *et al.* Diagnostic ability of wide-field retinal nerve Fiber layer maps using swept-source optical coherence tomography for detection of Preperimetric and early Perimetric glaucoma. *J. Glaucoma* **26**, 577–585 (2017).
- Yang, Z. *et al.* Diagnostic ability of retinal nerve Fiber layer imaging by swept-source optical coherence tomography in glaucoma. *Am. J. Ophthalmol.* **159**, 193–201 (2015).
- Yang, Z. *et al.* Diagnostic ability of macular ganglion cell inner plexiform layer measurements in glaucoma using swept source and spectral domain optical coherence tomography linden R, ed. *PLoS ONE* **10**, e0125957 (2015).
- Cvenkel, B., Sustar, M. & Perovšek, D. Monitoring for glaucoma progression with SAP, electroretinography (PERG and PhNR) and OCT. *Doc. Ophthalmol.* **144**, 17–30 (2022).
- Venkataraman, A. P. *et al.* Impact of optical coherence tomography scan direction on the reliability of peripapillary retinal nerve fiber layer measurements Bui BV, ed. *PLoS ONE* **16**, e0247670 (2021).
- Lee, S. Y. *et al.* Repeatability and agreement of swept source and spectral domain optical coherence tomography evaluations of thickness sectors in normal eyes. *J. Glaucoma* **26**, e46–e53 (2017).
- Chaglasian, M. *et al.* The development of a reference database with the Topcon 3D OCT-1 Maestro. *OPHTH* **12**, 849–857 (2018).
- Kelty, P. J. *et al.* Macular thickness assessment in healthy eyes based on ethnicity using stratus OCT optical coherence tomography. *Invest. Ophthalmol. Vis. Sci.* **49**, 2668 (2008).
- Knight, O. J. Effect of race, age, and axial length on optic nerve head parameters and retinal nerve Fiber layer thickness measured by cirrus HD-OCT. *Arch. Ophthalmol.* **130**, 312 (2012).
- Knighton, R. W. & Qian, C. An optical model of the human retinal nerve fiber layer: Implications of directional reflectance for variability of clinical measurements. *J. Glaucoma* **9**, 56–62 (2000).
- Alamouti, B. Retinal thickness decreases with age: An OCT study. *Br. J. Ophthalmol.* **87**, 899–901 (2003).

Acknowledgements

National Institutes of Health/National Eye Institute Grants R01EY029058, R01EY034148.

Author contributions

Study conception and design: H.H., M.K.D. Acquisition, analysis, and interpretation of data: H.H., N.W.E., M.K.D., and J.D.A. Draft manuscript: HH Substantive revision: H.H., N.W.E., M.K.D., S.M., and R.N.W. All authors reviewed the results and approved the final version of the manuscript.

Competing interests

Huiyuan Hou: Employment- Topcon; Nevin W. El-Nimri: Employment- Topcon; Mary K. Durbin- Employment- Topcon; Juan D. Arias: Employment- Topcon; Sasan Moghimi: none; Robert N. Weinreb: Research support-Centervue, Heidelberg Engineering, National Eye Institute, National Institute of Minority Health and Health Disparities, Optovue, Research to Prevent Blindness, Zilia; Consultant- Abbvie, Alcon, Allergan, Amydis, Editas, Eyeovia, Iantrek, Implantsdata, IOptic, iSTAR Medical, Nicox, Santen, Tenpoint, Topcon.

Additional information

Supplementary Information The online version contains supplementary material available at <https://doi.org/10.1038/s41598-023-43230-7>.

Correspondence and requests for materials should be addressed to H.H.

Reprints and permissions information is available at www.nature.com/reprints.

Publisher's note Springer Nature remains neutral with regard to jurisdictional claims in published maps and institutional affiliations.



Open Access This article is licensed under a Creative Commons Attribution 4.0 International License, which permits use, sharing, adaptation, distribution and reproduction in any medium or format, as long as you give appropriate credit to the original author(s) and the source, provide a link to the Creative Commons licence, and indicate if changes were made. The images or other third party material in this article are included in the article's Creative Commons licence, unless indicated otherwise in a credit line to the material. If material is not included in the article's Creative Commons licence and your intended use is not permitted by statutory regulation or exceeds the permitted use, you will need to obtain permission directly from the copyright holder. To view a copy of this licence, visit <http://creativecommons.org/licenses/by/4.0/>.

© The Author(s) 2023